

Supplementary Materials

Production of energy-storage paper electrodes using a pilot-scale paper machine

*Patrik Isacsson,^{a,d} Karishma Jain,^b Andreas Fall,^c Valerie Chauve,^d Alireza Hajian,^{2†} Hjalmar Granberg,³
Lucie Boiron,^d Magnus Berggren,^{a,f} Karl Håkansson,^c Jesper Edberg,^e Isak Engquist,^{a,f*} Lars Wågberg^{b,g*}*

^a *Laboratory of Organic Electronics, Department of Science and Technology, Linköping University, 601 74 Norrköping, Sweden*

^b *Department of Fiber and Polymer Technology, KTH Royal Institute of Technology, Teknikringen 56–58, SE-100 44 Stockholm, Sweden.*

^c *RISE Research Institutes of Sweden, Bioeconomy and Health, SE-114 86 Stockholm, Sweden.*

^d *Ahlstrom-Munksjö Research Center, 38140 Apprieu, France.*

^e *RISE Research Institutes of Sweden, Digital Systems, Bio- and Organic Electronics, Bredgatan 35, Norrköping SE-602 21, Sweden.*

^f *Wallenberg Wood Science Center, Linköping University, Department of Science and Technology, Linköping University, 601 74 Norrköping, Sweden.*

^g *Wallenberg Wood Science Center, KTH Royal Institute of Technology, Teknikringen 56–58, SE-100 44 Stockholm, Sweden.*

[†] *Present address: Department of Mechanical Engineering, Massachusetts Institute of Technology, 77 Massachusetts Avenue, Cambridge, MA 02139, USA*

** Corresponding authors*

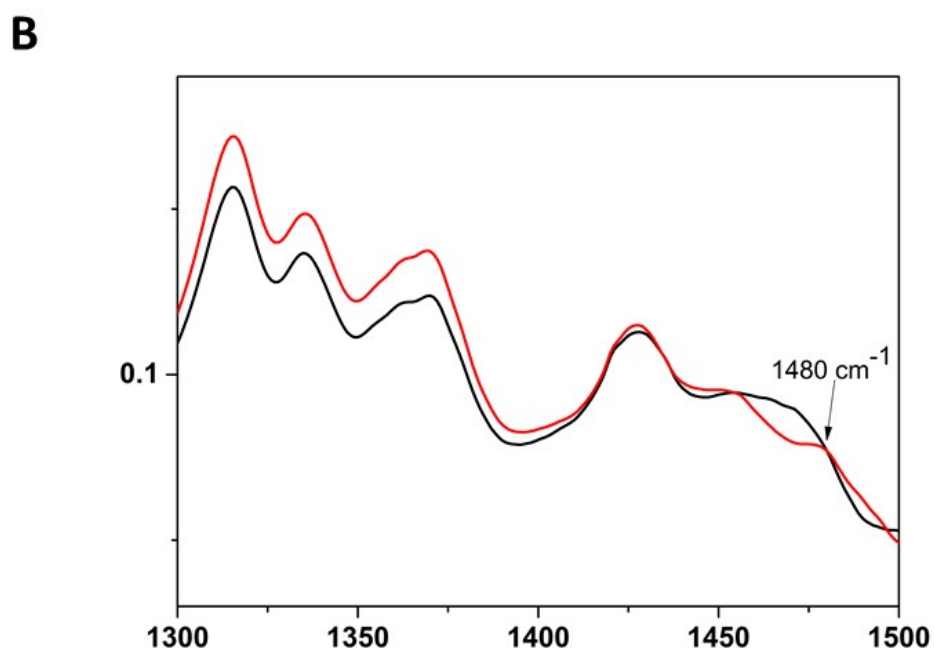
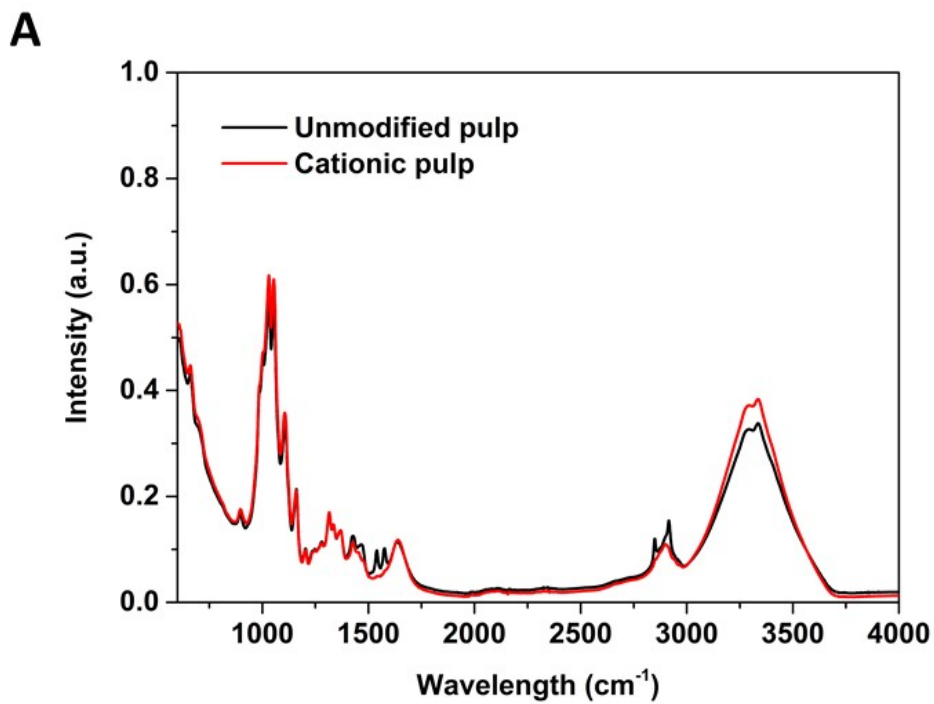


Figure S1. FTIR spectra of unmodified (black) and cationized (red) fibers. The peak at 1480 cm^{-1} visible in the enlarged graph (B) is representative of methyl groups in trimethyl ammonium, which shows the presence of trimethylammonium groups on cationic fibers.

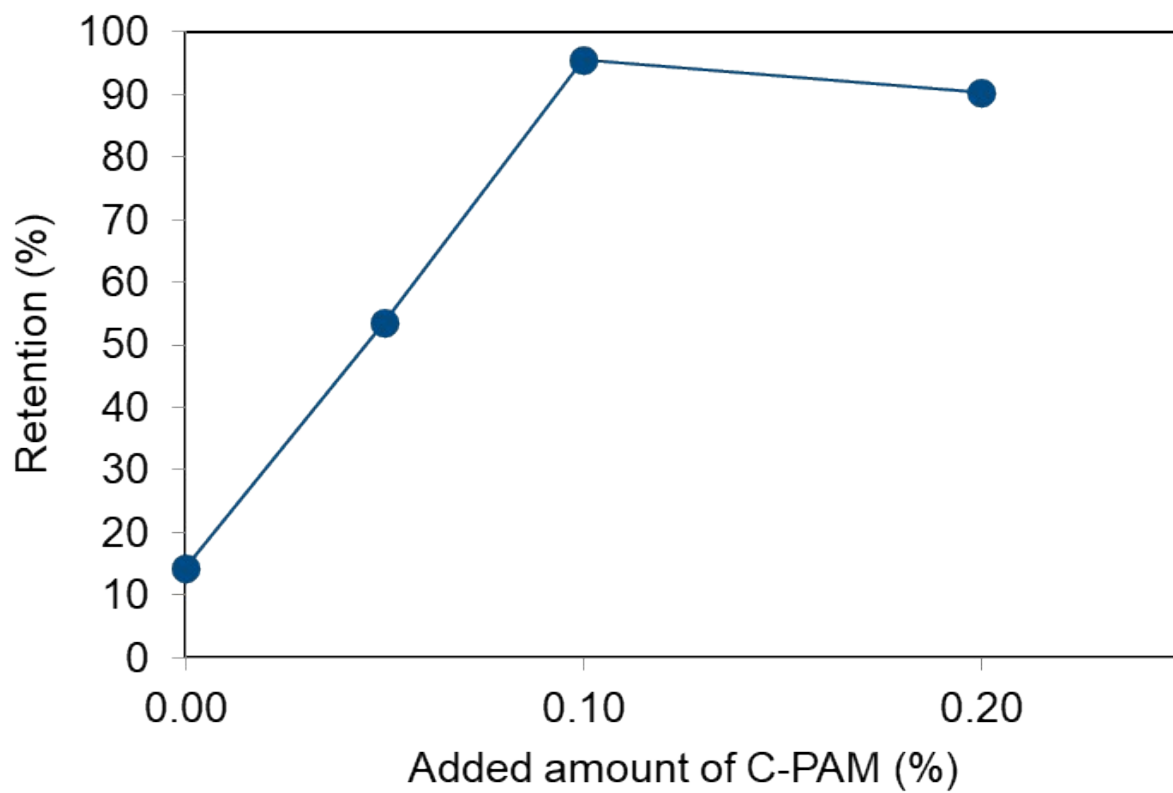


Figure S2. Results of retention trial. In the system consisting of an aqueous suspension of PEDOT:PSS-adsorbed cationic cellulose-rich fibers, activated carbon and cationic polyacrylamide (C-PAM), the total retention peaks at 0.10 wt% C-PAM.

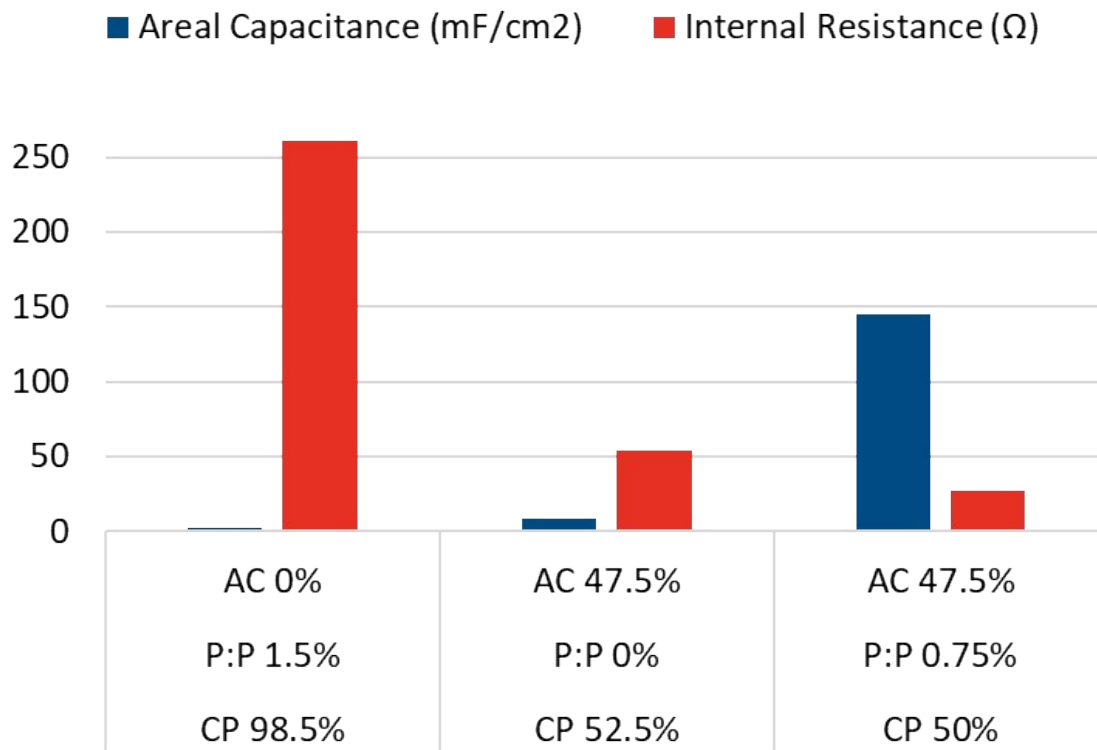


Figure S3. Areal capacitance and internal resistance of paper electrode handsheets measured in a 3-electrode setup with 1M KCl electrolyte, galvanized steel mesh as counter electrode and Ag/AgCl as reference electrode. The combination of cationic pulp (CP) with adsorbed PEDOT:PSS (P:P) and activated carbon (AC) improves both the internal resistance and areal capacitance.

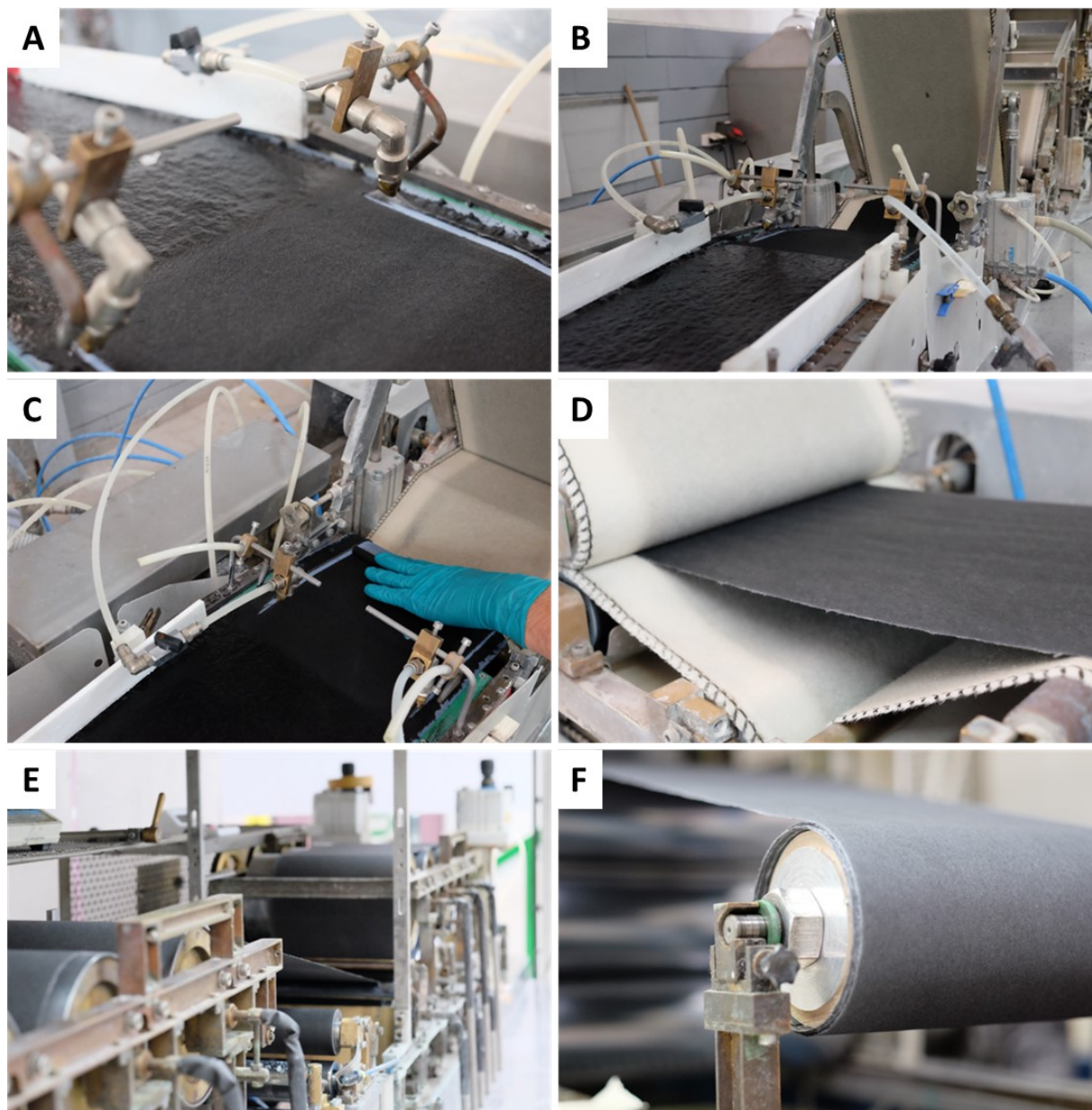


Figure S4. Photographs of the pilot line during the paper electrode trial. (A) view of the forming section, showing the dry line and the waterjet cutters, (B) forming section view towards pressing section, (C) manual transfer from the forming to the pressing section, (D) paper coming out from the pressing section, (E) view from the first drying section towards the second, (F) ready electrode paper being winded on the pilot tambour.

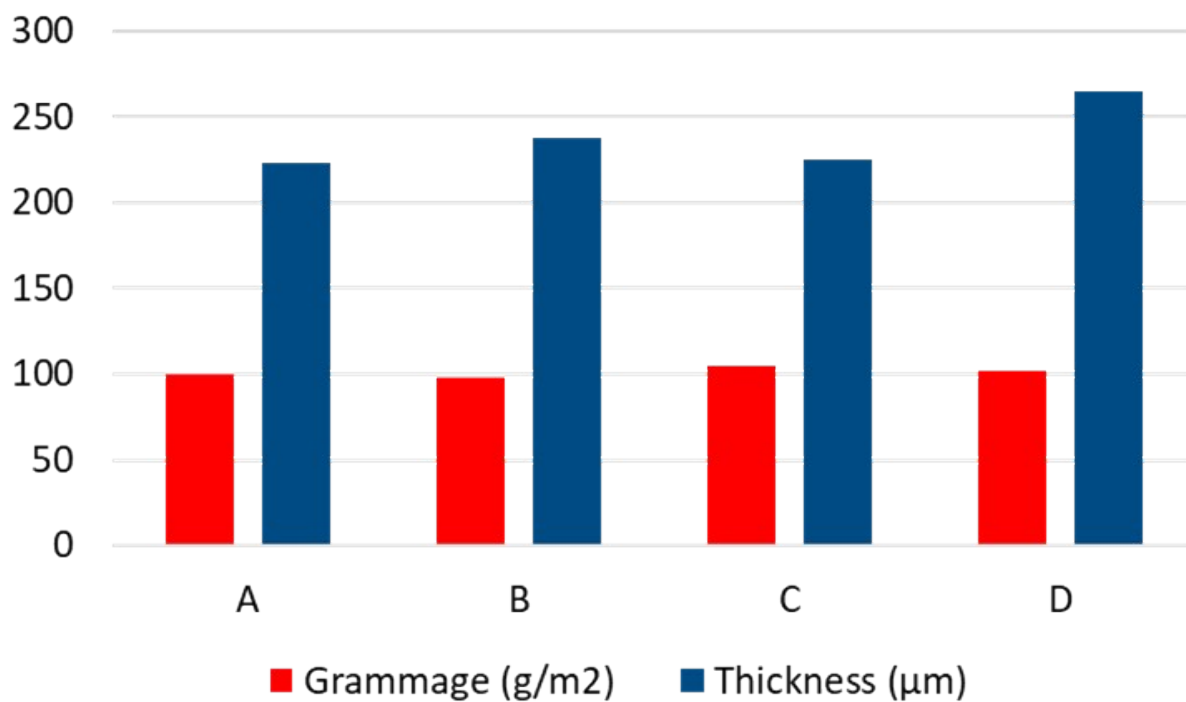


Figure S5. Grammage and thickness of the pilot machine-produced papers. The letters correspond to the different formulations; (i) = without CNF nor CB:CNF, (ii) = with CNF but without CB:CNF, (iii) = without CNF but with CB:CNF and (iv) = with both CNF and CB:CNF.

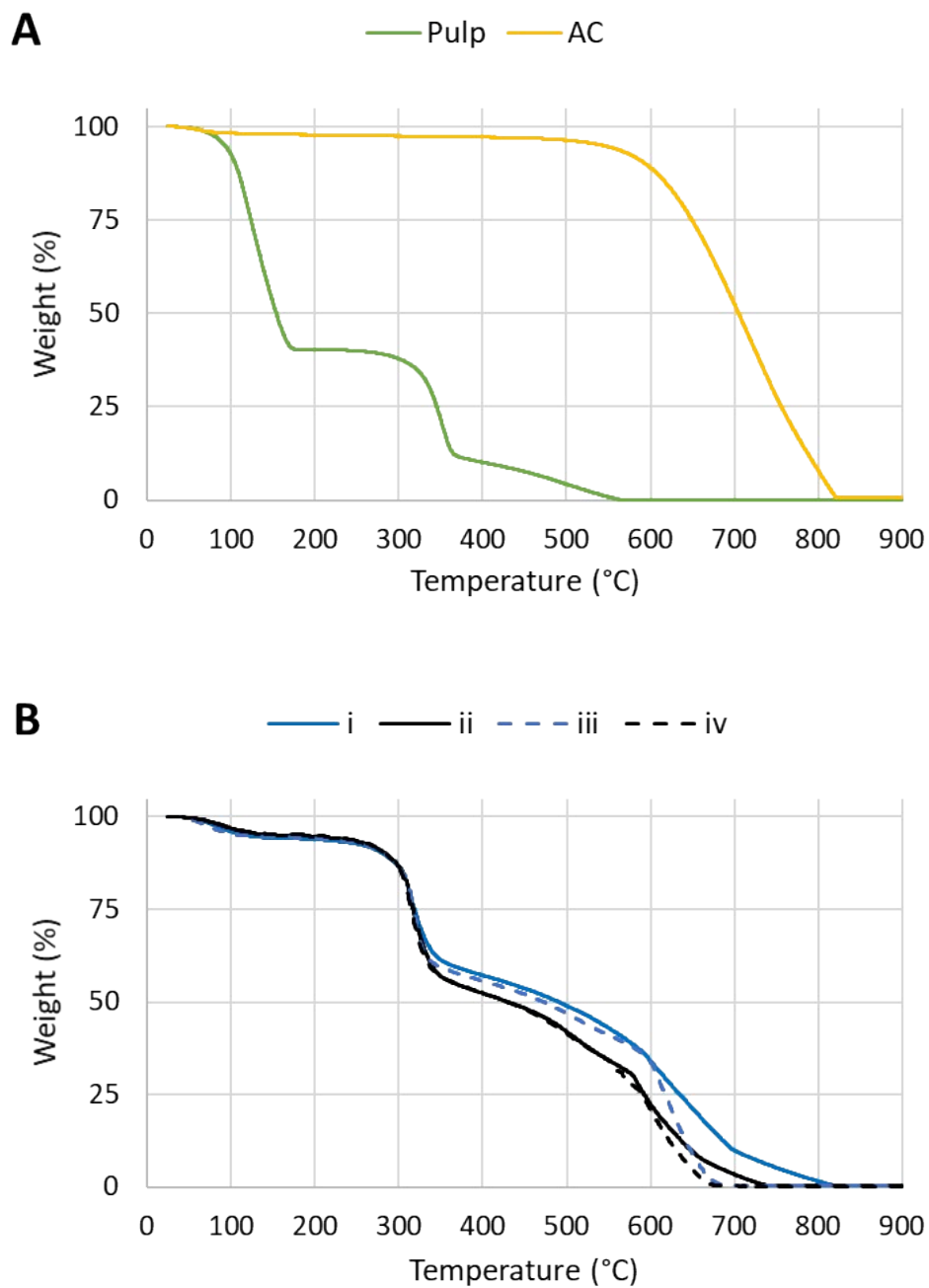


Figure S6. TGA results for the main components pulp and activated carbon (A) and for the papers i-iv (B). The large mass loss for pulp until 180°C in (A) is attributed to evaporation of water.

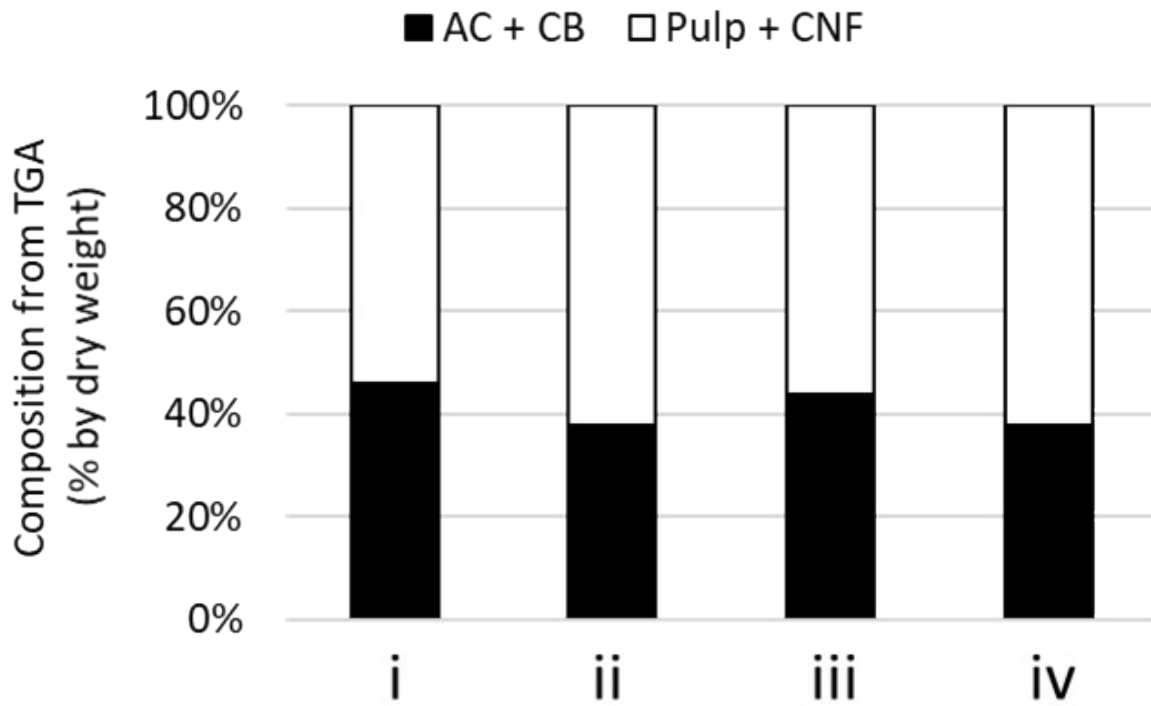


Figure S7. Paper composition as determined by TGA shows a lower loading of AC in the papers from formulation (ii) and (iv), where CNF has been used as an additive.

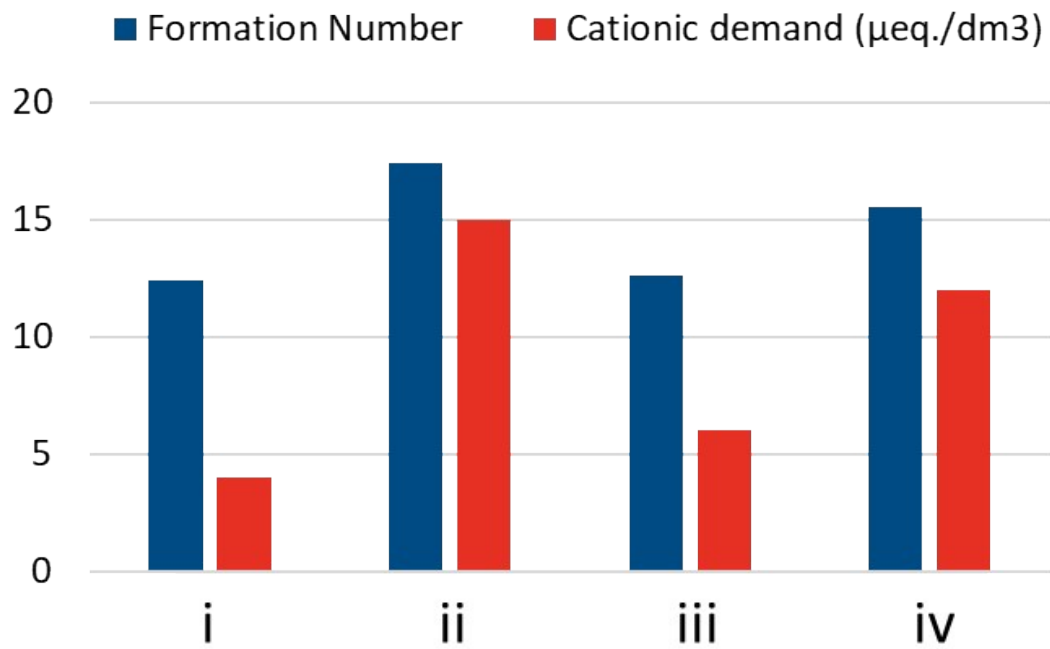


Figure S8. Papers from formulation (ii) and (iv), where CNF has been used as an additive, display poorer formation (i.e. higher formation numbers) as well as higher cationic demand of the white-water phase.

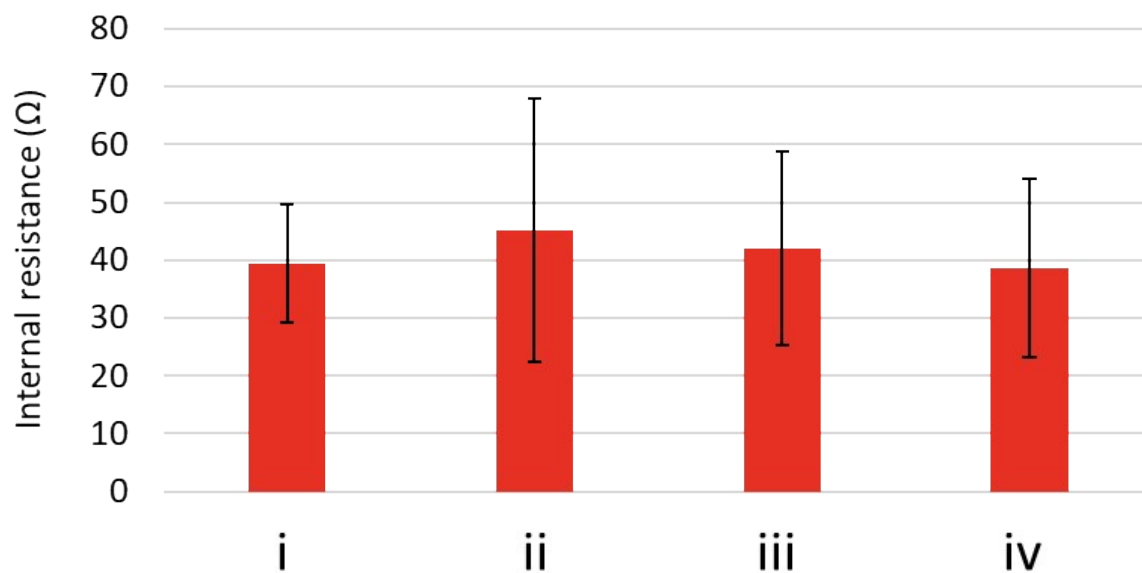


Figure S9. Internal resistance of the pilot machine-produced papers measured in a 3-electrode setup with 1M KCl electrolyte, activated carbon felt as counter electrode and Ag/AgCl as reference electrode. The letters correspond to the different formulations; (i) = without CNF nor CB:CNF, (ii) = with CNF but without CB:CNF, (iii) = without CNF but with CB:CNF and (iv) = with both CNF and CB:CNF.

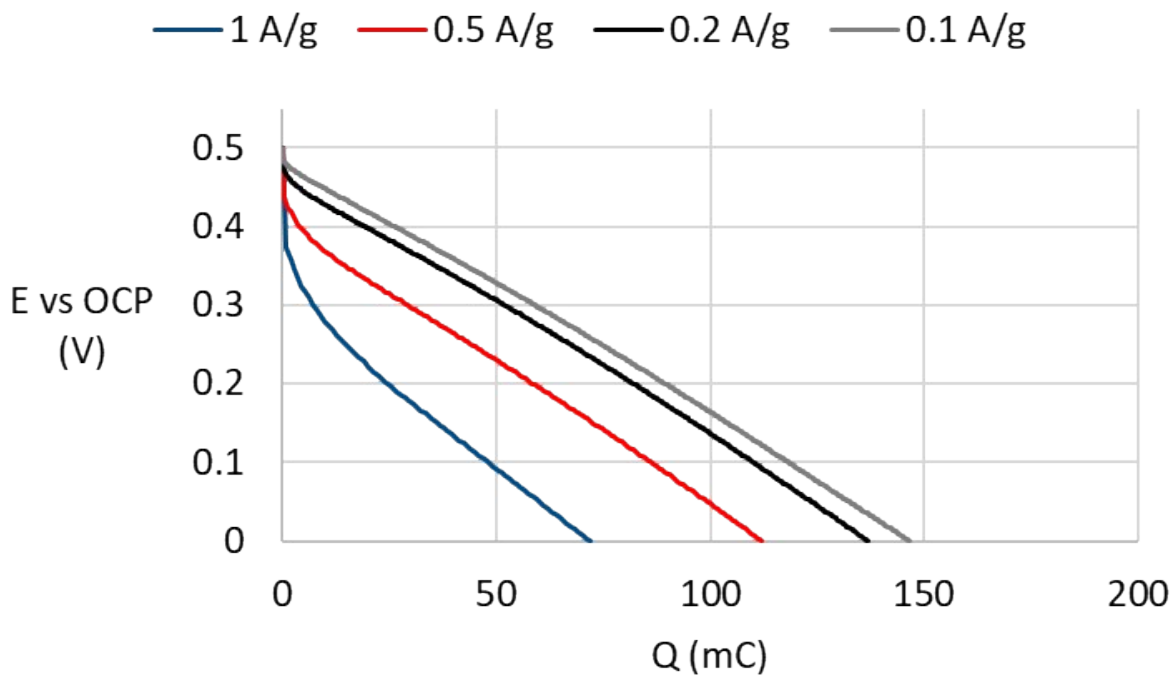


Figure S10. Discharge of paper (i) (without CNF nor CB:CNF) in a 3-electrode setup with 1M KCl electrolyte, galvanized steel mesh as counter electrode and Ag/AgCl as reference electrode. The open circuit potential (OCP) vs Ag/AgCl was used as the starting point for the measurements.

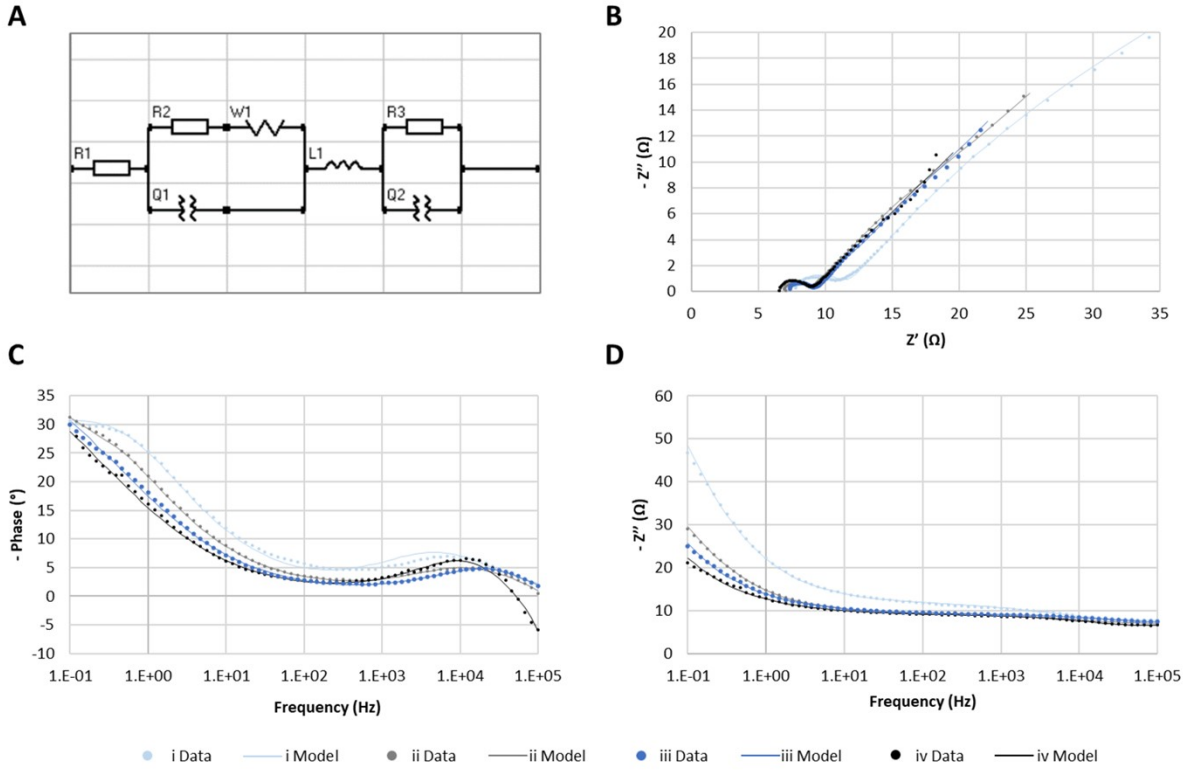


Figure S11. Results from electrochemical impedance spectroscopy (EIS) analysis of papers i-iv. The equivalent circuit (A) gave a good model fit to the EIS results of the papers, demonstrated in Nyquist (B) and Bode (C, D) plots.

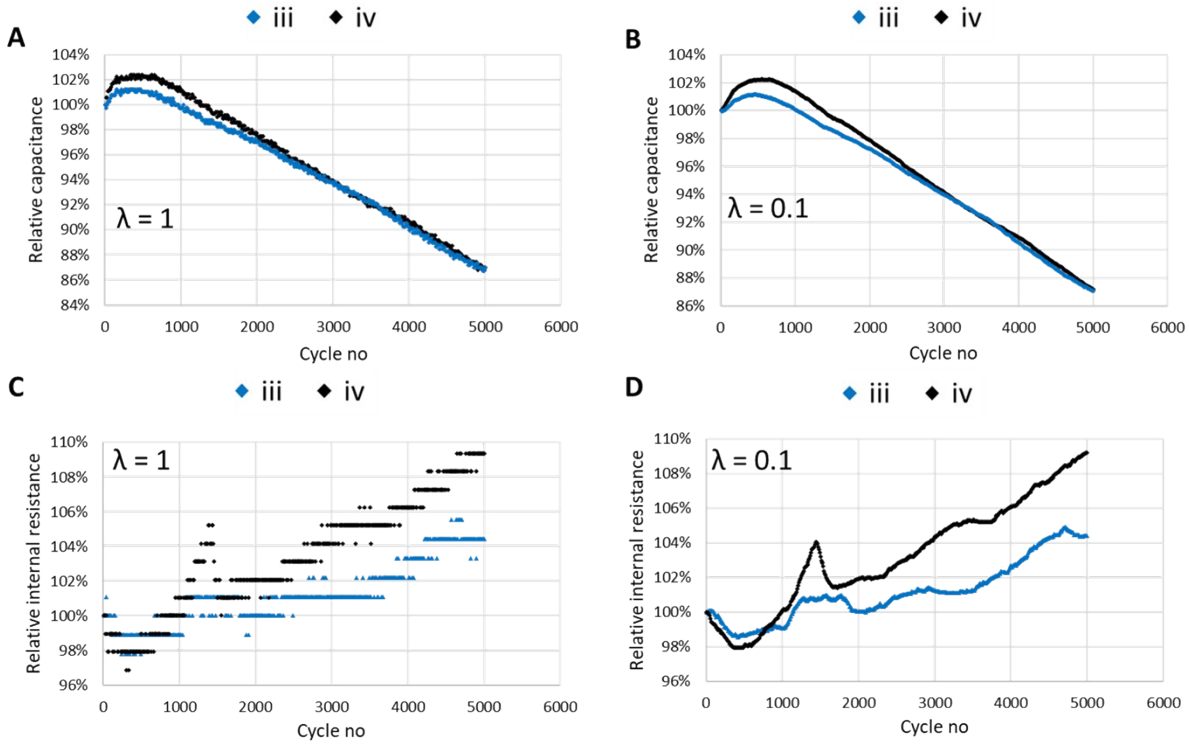


Figure S12. Relative capacitance (A, B) and relative internal resistance (C, D) derived from each 10th discharge over 5'000 cycles for the papers iii and iv with a discharge rate at 1 A/g activated carbon in a 3-electrode setup with 1M KCl electrolyte, platinum mesh as counter electrode and Ag/AgCl as reference electrode. The open circuit potential (OCP) vs Ag/AgCl was used as the starting point for the measurements.

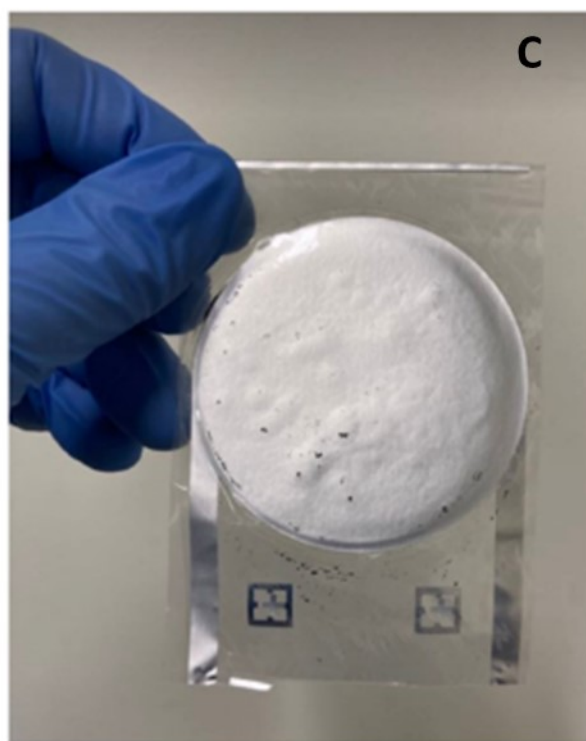
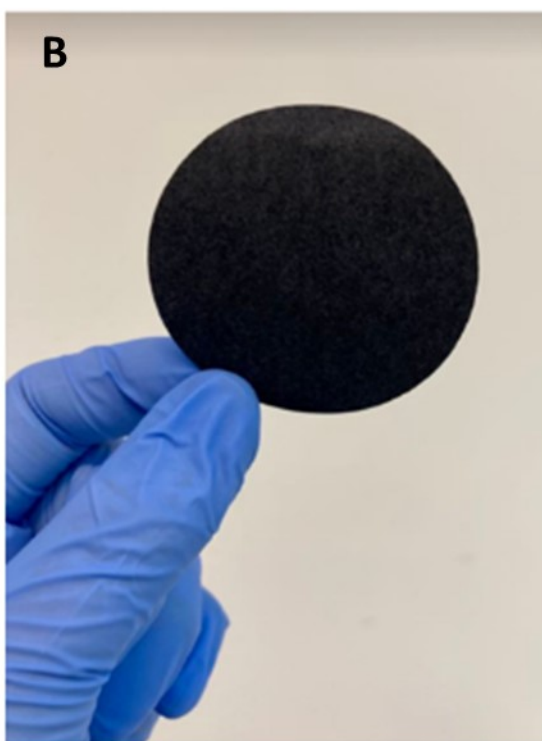
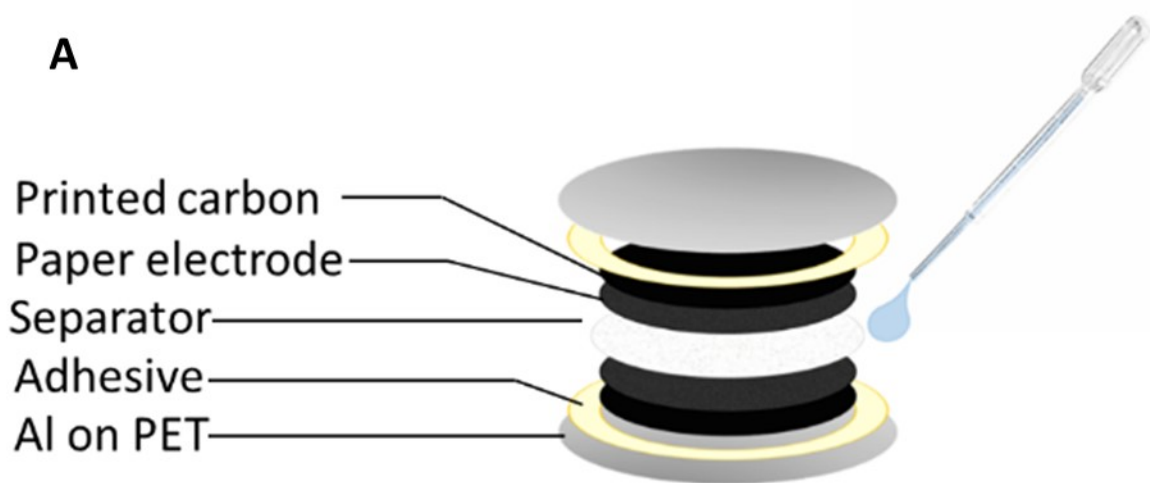


Figure S13. Assembling of the EDLC device. (A) Schematic of the supercapacitor device, (B) photos of the cut electrode paper from formulation (iii) and (C) the assembled EDLC cell.